UBE2S Activates NF-κB Signaling By Binding With IκBα and Promotes Metastasis of Lung Adenocarcinoma Cell

Jhih-Yun Ho
Taipei Medical University
Hsing-Hsien Cheng
Taipei Medical University
Yu-Chieh Kuo
Taipei Medical University
Yu-Lin A. Lee
Duke University Hospital
Chia-Hsiung Cheng (chcheng@tmu.edu.tw)
Taipei Medical University https://orcid.org/0000-0003-0307-9650

Research

Keywords: UBE2S, IκBα, NF-κB, metastasis, lung adenocarcinoma

Posted Date: April 19th, 2021

DOI: https://doi.org/10.21203/rs.3.rs-409169/v1

Version of Record: A version of this preprint was published at Cellular Oncology on September 28th, 2021.
See the published version at https://doi.org/10.1007/s13402-021-00639-4.

Abstract

Background

Nuclear factor (NF)-κB signaling in cancer cells was reported to be involved in tumorigenesis. Phosphorylation and degradation of inhibitor of NF-κBα (IκBα) is a canonical pathway of NF-κB signaling. Herein, we report non-canonical activation of NF-κB signaling without phosphorylation of IκB but by directly binding by ubiquitin-conjugating enzyme E2S (UBE2S) for degradation in adenocarcinoma cells.

Methods

TCGA and the Human Atlas Protein Database were used to analyze the survival rate and expression of UBE2S. PC9, H460, H441 and A549 cells were used in this study. PC9 and H460 cells were used for further analysis because of different protein levels of UBE2S. Specific IKK inhibitors, PS1145 and SC514, were used to analyze the phosphorylation of IκBα. Western blotting experiment was used to analyze the protein levels PC9 and H460 cells. Wound-healing experiment was used to analyze the migrative ability of PC9 and H460 cells. Overexpression and knockdown of UBE2S in H460 and PC9 cells were used to analyze the downstream proteins levels. Immunoprecipitation, immunofluorescent staining, a glutathione S transferase (GST) pull-down assay, and an in vitro binding assay were used to analyze the interaction of UBE2S and IκBα. Luciferase assay was used to analyze the activation of NF-κB signaling regulated by UBE2S. Zebrafish xenograft model was used analyzed the metastasis of PC9 cells regulated by UBE2S.

Results

UBE2S in lung adenocarcinoma patients was negatively related to the survival rate. The protein levels of UBE2S and IκBα were shown opposite change in PC9 and H460 cells. PC9 cells showed higher UBE2S expression and migrative ability than H460 cells. Phosphorylation of IκBα was not changed by treatment with IKK specific inhibitors, PS1145 and SC514, in PC9 and H460 cells. Overexpression and knockdown of UBE2S in H460 and PC9 cells showed the protein levels of IκBα were regulated. Immunoprecipitation, immunofluorescent staining, a glutathione S transferase (GST) pull-down assay, and an in vitro binding assay showed the direct binding of UBE2S with IκBα. Protein levels of nuclear p65 and luciferase assay showed the NF-κB signaling was regulated UBE2S. EMT markers and migrative ability of cancer cells were also regulated by UBE2S. Zebrafish xenograft tumor model showed the reduction of migrative PC9 cells by knockdown of UBE2S.

Conclusion

Higher UBE2S expressed in lung adenocarcinomas could bind with IκBα for activation of NF-κB signaling to promote metastasis of cancer cells. UBE2S might be a potential therapeutic target for lung adenocarcinomas.

Background

The ubiquitin-conjugating enzyme E2S (UBE2S) ubiquitin carrier protein is an E2 ubiquitination ligase that helps the E1, E2, and E3 ligases link ubiquitin with target proteins, which then targets them towards proteasome degradation [1-3]. The ubiquitin-proteasome pathway was documented to play critical roles in tumor formation and progression [4]. The extent of UBE2S, which is highly expressed in several types of tumors, was correlated with the progression of tumors in esophageal cancer patients [5], breast tumors tissues [6], lung tumor cells [7], papillary renal cell carcinoma [8], endometrial tumors [9], glioblastoma multiforme [10], and colon cancer development [11]. UBE2S was suggested to be a potential biomarker for diagnostic, prognostic, and therapeutic targets [12]. UBE2S is involved in stabilization of hypoxia-inducible factor (HIF)-1α-induced tumorigenesis [13]. UBE2S was also reported to be overexpressed in lung cancer [7, 14]. Nuclear factor (NF)-κB expression was related to the tumor stage, lymph node metastasis, and 5-year overall survival rate for non-small cell lung cancer patients [15].

NF-κB is constitutively activated in some types of cancer cells and is able to induce several aspects of tumorigenesis, including proliferation, anti-apoptosis, angiogenesis, and metastasis [16]. Activation of NF-κB is generally involved in phosphorylation of inhibitor of NF-κBα (IκBα) by IκB kinase (IKK) for degradation. NF-κB is then translocated from the cytoplasm into nuclei. It binds to the promoter region of target genes with specific site-activated transcription of target genes related to cell proliferation [17], anti-apoptosis [18, 19], drug resistance [20], angiogenesis, and metastasis [21, 22]. Low IκBα and high constitutive NF-κB activities were reported in adenocarcinoma cells and induced only weak NF-κB activity by tumor necrosis factor (TNF)-α treatment [23]. Stabilization of free IκB is not regulated by IKK but is related to the proline (P), glutamic acid (E), serine (S), threonine (T) (PEST) domain and proteasome degradation [24]. Degradation of IκBα to activate NF-κB signaling in cancer cells without IKK activation might play an important role in tumorigenesis.

In our earlier reports, metastasis of tumor cells was activated by matrix metalloproteinase (MMP)-9 through epithelial-to-mesenchymal transition (EMT) signaling [25-30]. Snail and MMP-9 are downstream target genes of NF-κB [31]. We also found that acceleration of nuclear entry of NF-κB activated expression of EMT markers in A431-III cells [32]. Treatment with the dietary flavonoids, luteolin and quercetin, was able to inhibit stemness, reactive oxygen species (ROS), and the invasive capacity of A431-III cells by reducing the EMT and inhibiting the phosphorylation of Akt and glycogen synthase kinase-3β (GSK3β) [32-34]. UBE2S is highly expressed and promotes the migratory and invasive abilities of cancer cells [28]. UBE2S is stabilized by Akt phosphorylation and is involved in DNA repair mechanisms by degradation of the Ku70 complex [10]. Akt might stabilize UBE2S by phosphorylation and mediate NF-κB signaling to promote metastasis of cancer cells.

In this study, we investigated the interaction and effects of UBE2S with IκBα on lung cancer cells. The binding ability of UBE2S with IκBα was analyzed by immunoprecipitation (IP) and in vitro pull-down assays. Protein levels of UBE2S and IκBα were analyzed in lung cancer cells. Knockdown and

overexpression of UBE2S in lung cancer cells were performed to analyze protein levels of IκBα and EMT markers.

Methods

Chemicals and reagents

Dulbecco's modified Eagle medium (DMEM), RPMI-1640, 0.25% trypsin, Ly294002, and fetal bovine serum (FBS) were obtained from ThermoFisher Scientific (Cleveland, OH, USA). MG132, S3I-201, DMSO, paraformaldehyde (PFA), lysogeny broth (LB), MS222, isopropyl β- d-1-thiogalactopyranoside (IPTG), and 3-(4,5-dimethylthiazol-2-yl)-2,5-diphenyl tetrazolium bromide (MTT) were purchased from Sigma-Aldrich (Merck, Darmstadt, Germany). Protein G Mag Sepharose, glutathione Sepharose 4B GST-tagged protein purification resin, Ni Sepharose high-performance histidine-tagged protein purification resin, and Amicon ultra-centrifugal filters were obtained from GE (Marlborough, MA, USA). Primers were purchased from Purigo Biotech (Taipei, Taiwan). KAPA HiFi polymerase chain reaction (PCR) kits were purchased from Roche (Wilmington, MA, USA). PolyJet was purchased from SignaGen Laboratories (Rockville, MD, USA). The luciferase assay reagent was purchased from Promega (Madison, WI, USA). Anti-UBE2S, anti-lamin-A, and anti-GAPDH antibodies were obtained from GeneTex (Irvine, TX, USA). The p65 antibody was acquired from Cell Signaling Technology (Danvers, MA, USA). Anti-IκBα, anti-phosphorylated (p)-IκBα, anti-matrix metalloproteinase (MMP)-9, anti-Twist, and anti-E-cadherin (E-Cad) antibodies were obtained from Abcam (Cambridge, UK). Anti-hemoagglutinin (HA), anti-flag, anti-His, and anti-β-glutathione S-transferase (GST) antibodies were purchased from Santa Cruz (Capitola, CA, USA).

Database

The survival rate of lung adenocarcinoma patients correlated with UBE2S mRNA was analyzed by GEPIA2 web site (http://gepia2.cancer-pku.cn) [35]. The protein level of UBE2S in lung cancer patients was obtained from staining with CAB015228 antibody in the Human Atlas Protein Database (https://www.proteinatlas.org) [36].

Cell culture

The H441, A549, PC9, and H460 human lung cancer cell lines were obtained as described previously [52]. PC-9 and H460 cells were incubated with RPMI-1640 medium containing 10% FBS (ThermoFisher Scientific) in a 5% CO_2 atmosphere at 37 °C.

Plasmid construction

The pcDNA3-UBE2S-flag plasmid was obtained as described in our earlier report [28]. pCMV4-3 HA/IκBα was purchased from addgene (Cambridge, MA, USA). The coding region of *IκBα* was amplified by a KAPA HiFi PCR Kit (Roche) and cloned to the pcDNA3-HA vector as the pcDNA3-IkBa-HA plasmid. The pcDNA3-IkBa-flag plasmid was digested with *Bam*HI and *Sal*I and inserted into the PQE30 vector as the PQE30-

IkBa plasmid. The pcDNA3-UBE2S-flag plasmid was digested with *Bam*HI and *Xho*I and inserted into the pGEX-4T-2 vector as the pGEX-UBE2S plasmid. The following primer pairs were used for the PCR: IκBα-forward (5'-ATG TTC CAG GCG GCC G-3') and IκBα-reverse (5'-TAA CGT CAG ACG CTG G-3').

Cell viability assay

H460 and PC-9 cells (10^5 cells/well) were seeded in 48-well plates overnight. PC-9 cells were treated with DMSO, SC514, PS1145, and Ly294002 for 24 h. Cells were refreshed with culture medium with 5 mg/mL of MTT (Merck), and incubation continued at 37 °C for 3 h. The culture medium was removed, and 200 μl DMSO was added to resolve precipitation. The absorbance was measured at 570 nm using a Spark multimode microplate reader (TECAN, Männedorf, Switzerland).

Preparation of cell lysates

Cultured cells were washed three times with phosphate-buffered saline (PBS). Gold lysis buffer (20 mM Tris-HCl at pH 7.9, 1 mM EGTA, 0.8 % NaCl, 0.1 mM β-glycerylphosphate, 1 mM sodium pyrophosphate, 10 mM NaF, 1 mM $Na_4P_2O_7$, 1 mM Na_3VO_4, 10% glycerol, 1% Triton X-100, 1 mM PMSF, 10 μg ⁄mL aprotinin, and 10 μg ⁄mL leupeptin) was used to lyse cells. The total cell lysate was collected by centrifugation at 14,000 *g* for 20 min at 4 °C and quantified by a Bio-Rad protein assay kit (Bio-Rad, Hercules, CA, USA). Cultured cells in 10-cm cultural plates were harvested, and nuclear extracts were collected using a mini-preparation method [53-56].

Western blotting

Protein samples were heated to 100 °C with sample buffer (250 mM Tris-HCl at pH 6.8, 10% sodium dodecylsulfate (SDS), 30% glycerol, 5% β-mercaptoethanol, and 0.02% bromophenol blue) for 5 min. SDS-polyacrylamide gel electrophoresis (PAGE) was used to separate proteins, which were then transferred to polyvinylidene difluoride (PVDF) membranes (Millipore, Billerica, MA, USA). After blocking with 3% bovine serum albumin (BSA) for 30 min at room temperature, a specific primary antibody diluted in 3% BSA was incubated with the membrane on a shaker at 4 °C overnight. The membrane was washed with PBST (0.25% Tween-20 in PBS) three times, and the secondary antibody conjugated with horseradish peroxide (Millipore) was incubated for 1 h at room temperature. After washing with PBST three times, proteins were detected using an enhanced chemiluminescence (ECL) reagent kit (Millipore) followed by exposure to Amersham Imager 600 imagers (GE). Protein images were quantified using ImageJ software (http://rsb.info.nih.gov/ij/index.html, National Institutes of Health, Bethesda, MA, USA).

Immunostaining

COS-1 cells (10^5 cells/well) were seeded onto 12-well plates overnight. The pcDNA3-UBE2S-HA and pcDNA3-IkBa-flag plasmids were transfected into COS-1 cells by PolyJet (SignaGen) for 24 h. PFA at 4% was used to fix COS-1 cells for 20 min, and PBST (0.1% Triton X-100 in PBS) was used to permeabilize them for 10 min. After being washed with PBS three times and blocking with 3% BSA for 1 h at room temperature, anti-HA and anti-flag monoclonal antibodies were incubated at 4 °C overnight. Cy3 AffiniPure goat anti-mouse immunoglobulin G (IgG) was added, incubated for 30 min, and then stained with 0.1% DAPI for 5 min. Images were captured with an Olympus IX70-FLA inverted fluorescence microscope (Olympus, Tokyo, Japan) and SPOT system (Diagnostic Instruments, Sterling Heights, MI, USA).

Knockdown of UBE2S by small interfering (si)RNA

UBE2S and control siRNAs were purchased from ThermoFisher Scientific and prepared following the manufacturer's instructions. In total, 10^6 cells were seeded onto six-well plates overnight and then transfected with 40 nM of siRNA using the GenMute siRNA transfection reagent (SignaGen Laboratories, Rockville, MD, USA) following the manufacturer's instructions. All assays were performed 24 h after transfection.

Luciferase assay

Cells (10^5) were seeded onto 12-well plates overnight. The pGL3-5xκB-Luc and pcDNA3-UBE2S-flag plasmids were obtained as described in our earlier reports [28, 57]. The pGL3-Basic, pGL3-5xκB-Luc, control siRNA, UBE2S siRNA, and pcDNA3-UBE2S-flag plasmids were transfected into H460 and PC9 cells using the PolyJet transfection reagent (SignaGen Laboratories) according to the manufacturer's instructions. Total cell lysates were collected at 48 h post-transfection. Luciferase activity was monitored with the Luciferase Assay Reagent (Promega) and detected by a Spark multimode microplate reader (Tecan, Mannedorf, Switzerland).

Expression and purification of GST-UBE2S and His-IκBα protein in *Escherichia coli*

PQE30-IκBα and pET4T2-UBE2S were transformed into *E. coli* DH5a strands and expressed by 0.2 M IPTG induction. Cells grown overnight were re-grown in 1/10 dilution of lysogeny broth (LB) for 1 h and inducted by 0.2 M IPTG for 3 h. Cells were collected by centrifugation and resuspended in cold GST buffer (50 mM Tris-HCl at pH 7.5, 150 mM NaCl, 1 mM EDTA, and a proteinase inhibitor cocktail) and His binding/wash buffer (0.5 M NaCl, 100 mM HEPES, 10 mM Imidazole at pH 8.0, 0.5% NP-40, 1 mM PMSF, and a proteinase inhibitor cocktail). Cells were processed by an Untrasonic Processors (Chrom Tech, Apple Valley, MN, USA) on ice. The lysate was centrifuged at 13,000 *g* for 10 min at 4 °C. The supernatant was applied to a glutathione Sepharose 4B GST-tagged protein purification resin (GE) and Ni Sepharose high-performance histidine-tagged protein purification resin (GE). After being washed with GST wash buffer (0.5% Triton X-100 and 1 mM EDTAU in PBS) and His binding/wash buffer, GST-UBE2S was re-suspended in PBS. His-IκBα proteins were eluted with elution buffer (100 mM HEPES and 0.5 M imidazole at pH 8.0), followed by changing the buffer to PBS by Amicon Ultra Centrifugal Filters (GE).

Pull-down and *in vitro* binding assays

For the pull-down assay, GST-UBE2S proteins on beads were added to the total lysate of H460 cancer cells and incubated at 4 °C overnight on a rolling shaker. After centrifugation at 500 *g* for 2 min and washing three times with PBS, the beads were resuspended in PBS and analyzed by Western blotting. The in vitro binding assay was performed by mixing equal volumes of GST-UBE2S and the IκBα protein to interact at 4 °C overnight on a rolling shaker. After centrifugation at 500 *g* for 2 min and washing three times with PBS, the beads were resuspended in PBS and analyzed by Western blotting.

Immunoprecipitation (IP)

Cultured cells in 10-cm plates were collected and treated with IP-lysis buffer (150 mM NaCl, 20 mM NaCl, 20 mM HEPES at pH 7.2, 10 mM NaF, 1 mM EDTA, 1% NP-40, 1 mM Na3V04, 1 mM PMSF, 1 DTT, and a proteinase inhibitor cocktail) for 10 min. Total cell lysate was collected by centrifugation at 13,000 rpm for 10 min. Pretreatment with protein G Mag Sepharose magnetic beads (GE) for 1 h was used to collect total proteins. An anti-UBE2S (GeneTex) or anti-IκBα (Abcam) monoclonal antibody was coated onto protein G Mag Sepharose magnetic beads (GE) for 1 h and washed with PBS three times. Coated protein G Mag Sepharose magnetic beads (GE) were added to total cell lysates, and the complex was pulled-down overnight. After washing with PBS three times, the protein G Mag Sepharose complex was immunoblotted with an anti-UBE2S (GeneTex) or anti-IκBα (Abcam) monoclonal antibody.

Cell migration assay

PC9 cells ($5x10^5$ cells/well) were plated onto six-well culture plates overnight in RPMI-1640 containing 10% FBS. Monolayer cells were scratched with a pipette tip. After washing with PBS, the monolayers were incubated at 37 °C for 24 h. Images of the monolayers were captured at 0 and 24 h using a phase-contrast Zeiss Axio Vert.A1 inverted microscope (Zeiss, Jena, Germany) and a Leadview 2800AM-FL camera (Leadview, Taipei, Taiwan). Migrating cells were calculated from triplicate determinations for each treatment group.

Zebrafish metastasis model

Zebrafish (Danio rerio) and embryos were maintained at 28 °C. All animal procedures were approved by the Institutional Animal Care and Use Committee or Panel (IACUC/IACUP) (protocol # LAC-2019-0355). The methods were carried out in accordance with the approved guidelines. The migration assay of cancer cells in zebrafish was analyzed following our earlier report [30, 44]. Briefly, GFP expressing PC9 cells were transfected with control or UBE2S siRNA for 24h. The 0.25 % trypsin (ThermoFisher) was used to detach cancer cells and following stained with 1 μM CM-DiI (ThermoFisher) for 20 min. After 3 times wash with PBS, tumor cells were diluted as $2x10^6$ cells/mL with PBS. Tumor cells were microinjected into the yolk of 3 days post-fertilization (dpf) zebrafish larvae by IM300 Microinjector (Narishige, Tokyo, Japan) at 30 psi. Zebrafish larvae were then incubated at 28 °C for 1 h and then transferred to 32 °C for further incubation. The migrative tumor cells in zebrafish larvae were analyzed at 7 dpf zebrafish larvae using a phase-

contrast Olympus IX70 microscope (Olympus, Tokyo, Japan) and a SPOT camera (Sterling Heights, MI, USA).

Statistical analysis

Three independent experiments were used to analyze the mean ± standard deviation (SD). Statistical significance was analyzed by a one-way analysis of variation (AVOVA) followed by Tukey's test. Statistical significance was indicated by * $p < 0.05$, ** $p < 0.01$, and *** $p < 0.001$.

Results

UBE2S has an important role in clinical lung adenocarcinoma patients

To investigate the role of UBE2S in lung adenocarcinoma patients, The Cancer Genome Atlas (TCGA) database [35] and Human Protein Atlas database [36] were used to analyze messenger (m)RNA and protein levels of UBE2S. High levels of UBE2S mRNA were correlated with low survival rates in lung adenocarcinoma patients from TCGA database (Figure 1A). Strong and medium (MS) levels of the UBE2S protein were seen in 81.8% of lung adenocarcinoma patients compared to weak and normal (NW) levels by immunohistochemical (IHC) staining from the Human Protein Atlas database (Figure 1B). These results show that UBE2S might play an important role in tumorigenesis of lung adenocarcinomas.

UBE2S promotes tumorigenesis related to NF-κB signaling

To analyze the role of UBE2S in tumorigenesis of lung adenocarcinomas, we analyzed UBE2S expression levels in H441, A549, PC9, and H460 lung cancer cells. UBE2S was more highly expressed in PC9 cells than in H441, A549, and H460 cells (Figure 2A). In earlier reports, NF-κB signaling was suggested to be an important tumorigenesis and drug-resistance pathway in lung cancer [37-39]. UBE2S is an E2 ligase involved in K11-linked polyubiquitination of component proteins to promote NF-κB signaling in tumor cells [1, 40, 41]. UBE2S promotes proliferation and survival of lung adenocarcinoma cells [14]. To investigate the role of UBE2S in NF-κB signaling, we analyzed protein levels of UBE2S, IκBα, and phosphorylated (p)-IκBα in H460 and PC9 cancer cells which expressed different levels of UBE2S (Figure 2A). Protein levels of IκBα were higher in H460 than PC9 cells, which were opposite results than with UBE2S. Protein levels of p-IκBα were similar in these two cancer cells lines (Figure 2B). In a further analysis of p65 protein levels in the cytosol and nuclei, PC9 cells expressed higher p65 than H460 cells in the cytosol and nuclei (Figure 2C). A wound-healing experiment showed higher migratory abilities of PC9 than H460 cells (Figure 2D, E). Collectively, these results suggested that UBE2S might be involved in regulating tumorigenesis through NF-κB signaling without IKK activation in lung cancer cells.

UBE2S activates NF-κB signaling by targeting IκBα

In our present data, we found that expression levels of UBE2S and IκBα, but not p-IκBα, were opposite in H460 and PC9 cells. UBE2S is an E2 ligase and regulates degradation of proteins through polyubiquitination. To elucidate whether UBE2S regulates the degradation of IκBα and activates NF-κB

signaling to promote tumorigenesis, we treated PC9 cells with the IKK inhibitors, SC514 and PS1145, to reduce IκBα phosphorylation. Protein levels of p-IκBα did not significantly differ between the control and treatment groups (Figure 3A, B). In an earlier report, UBE2S was activated by Akt and could be inhibited by Ly294002 [10]. We found that UBE2S protein levels had decreased but IκBα had increased after treatment with 5 and 10 μM Ly294002 (Figure 3C). These data suggested that UBE2S might regulate activation of NF-κB signaling in PC9 cells without IKK-induced activation. To further analyze the interaction of UBE2S and IκBα, we knocked-down and overexpressed UBE2S in PC9 and H460 cells to analyze IκBα expression. We found that IκBα protein levels increased by knockdown with two UBE2S small interfering (si)RNAs in PC9 cells (Figure 3D). UBE2S overexpression in H460 cells showed that IκBα protein levels decreased in a dose-dependent manner (Figure 3E). Overexpression of UBE2S and treatment with MG132 in H460 cells retained IκBα protein levels (Figure 3F). Collectively, these results showed that UBE2S might target IκBα for degradation and promoted activation of NF-κB signaling.

Binding of UBE2S and IκBα

To identify whether UBE2S interacts with IκBα, we prepared an immunostaining experiment in COS-1 cells. The pcDNA3-UBE2S-flag and pcDNA3-IκBα -HA plasmids were transfected into COS-1 cells, and we analyzed localization of UBE2S (green) and IκBα (red) using anti-flag and anti-hemoagglutinin (HA) monoclonal antibodies. Expressions of UBE2S and IκBα in COS-1 cells were analyzed by Western blotting (Figure 4A). Immunostaining experiments showed that UBE2S and IκBα were co-localized in the cytosol (Figure 4B). In a further analysis of the interaction of UBE2S with IκBα, an IP experiment was carried out in H460 and PC9 cells. UBE2S was precipitated with IκBα in H460 and PC9 cells (Figure 4C). To investigate whether UBE2S directly binds IκBα, GST-tagged UBE2S (GST-UBE2S) and His-tagged IκBα (His-IκBα) were individually expressed and purified in an *Escherichia coli* expression system. Coomassie blue (CBB) staining and Western blot analysis using anti-GST and anti-UBE2S antibodies revealed the expression of GST-UBE2S (Figure 4D). His-IκBα expression was also detected by CBB staining and Western blotting using anti-His and anti-IκBα antibodies (Figure 4E). An in vitro pull-down assay was conducted to analyze the binding of UBE2S with IκBα in PC9 cells. GST-UBE2S in agarose beads was shown to pull-down IκBα in PC9 total cell lysate (Figure 4F). An in vitro binding assay was also conducted to elucidate the binding of UBE2 and IκBα. GST-UBE2S in agarose beads was shown to bind with the purified IκBα protein (Figure 4G). These data showed the direct binding of UBE2S with IκBα.

UBE2S activates NF-κB signaling and EMT signaling in lung adenocarcinoma cells

Earlier studies reported that EMT signaling was activated by NF-κB signaling [42]. In our present data, UBE2S directly bound to IκBα to degrade and promote activation of NF-κB signaling. To analyze UBE2S' regulation of activation downstream genes of NF-κB signaling, we prepared overexpression and knockdown experiments to analyze p65 expression in PC9 and H460 cells. UBE2S overexpression in H460 cells produced increased protein levels of p65 in the cytosol and nuclei (Figure 5A). UBE2S-knockdown in PC9 cells produced decreases in the p65 protein in the cytosol and nuclei (Figure 5B). We further prepared a luciferase report assay to analyze activation of NF-κB signaling by UBE2S in H460 and

PC9 cells. pGL3-5xκB-Luc plasmid DNA contains five repeats of κB-binding sites which are activated by NF-κB signaling. The transactivation activity increased 13-, 23-, and 35-fold after transfection with 0.25, 0.5, and 1 μg of pGL3-5xκB-Luc compared to pGL3-basic in H460 cells (Figure 5C). With the combined transfection with 0.5, 1, and 2 μg pcDNA3-UBE2S-flag and 0.5 μg of pGL3-5xκB-Luc plasmid DNA, the transactivation activity of pGL3-5xκB-Luc increased 1.4-, 1.8-, and 2.9-fold compared to the control group (pGL3-5xκB-Luc only) in H460 cells (Figure 5D). In PC9 cells, the transactivation activity of pGL3-5xκB-Luc increased 40-, 72.2-, and 81-fold after transfection with 0.25, 0.5, and 1 μg pGL3-5xκB-Luc compared to pGL3-basic (Figure 5E). UBE2S-knockdown with UBE2S siRNA (siUBE2S#1 and -#2) decreased the transactivation activity to 42% and 53% of that of the control group (control siRNA) (Figure 5F). These results show that UBE2S activated NF-κB signaling in lung adenocarcinoma cells. In our earlier report, we found that UBE2S promoted migration and invasion through EMT signaling in A431-III cells [28]. Collectively, UBE2S might activate NF-κB and EMT signaling in lung adenocarcinoma cells.

UBE2S promotes EMT signaling and metastasis of lung adenocarcinomas in zebrafish xenograft model

In our and others' reports, UBE2S activated EMT signaling in cancer cells [28, 43]. To investigate the function of UBE2S in metastasis of lung adenocarcinoma cells, we prepared a wound-healing experiment to analyze the migratory abilities of PC9 cells. UBE2S-knockdown by UBE2S siRNA (siUBE2S#1 and -#2) decreased the migratory abilities to 42% and 23% that of control siRNA (Con) in PC9 cells (Figure 6A, B). To investigate the function of UBE2S in activating EMT signaling in lung cancer cells, we prepared overexpression and knockdown of UBE2S in H460 and PC9 cells. UBE2S overexpression in H460 cells increased MMP-9 and TWIST protein levels. E-Cadherin (E-Cad) protein levels also decreased (Figure 6C). Knockdown of UBE2S by UBE2S siRNA (siUBE2S#1 and -#2) decreased MMP-9 and TWIST protein levels. In contrast, E-Cad protein levels increased (Figure 6D). These data suggested that UBE2S might promote EMT signaling in lung adenocarcinoma cells. In our earlier reports, zebrafish was shown as an efficient *in vivo* tumor cell migration model [30, 44]. To further investigate metastasis of lung adenocarcinoma cell *in vivo*, we prepared in vivo xenograft zebrafish model. PC9 cells was transfected with control (Con) and UBE2S siRNA (siUBE2S#1, #2) for 24 h. Tumor cells were collected and stained with CM-DiI (Figure 6Ca-b) and microinjected into yolk of 2 days post-fertilization (dpf) zebrafish larvae. The migrative tumor cells were identified at 3-dpf zebrafish larvae (Figure 6Cc-f). The metastatic tumor cells were significantly decreased to 32% and 33% compared to control group (Con) (Figure 6Cg). These results suggested that UBE2S might activate the metastasis of lung adenocarcinoma cells.

Discussion

This study reveals novel non-canonical activation of NF-κB signaling by UBE2S. NF-κB signaling was activated by UBE2S in lung adenocarcinoma cells without IKK-induced phosphorylation or degradation of IκBα. NF-κB and EMT signaling were activated by UBE2S. UBE2S in lung cancer patients was shown to be correlated with a poor survival rate in TCGA database. Contrasting simultaneous expressions of IκBα with UBE2S were observed and affected p65 accumulation in nuclei of lung adenocarcinoma cells. IκBα and p-IκBα protein levels were not affected by treatment with the specific IκB kinase (IKK) inhibitors, SC514

and PS1145, in PC9 cells, but they were reduced by treatment with Ly294002, which was reported to inhibit phosphorylation of UBE2S by Akt [10]. Knockdown and overexpression of UBE2S in PC9 and H460 cells also affected IκBα protein levels, accumulation of p65 in nuclei, and transactivation activity of the 5x-NF-κB-binding motif containing the promoter. EMT marker expressions were also regulated by UBE2S. Immunoprecipitation, immunostaining, in vitro pull-down, and in vitro binding assays showed the direct binding of UBE2S with IκBα. Collectively, we hypothesized novel non-canonical activation of NF-κB signaling in lung adenocarcinomas (Figure 7). In low-malignancy lung adenocarcinoma cells, low UBE2S expression failed to bind with IκBα for degradation. IκBα bound with p65 and p50. Weak IKK signaling was activated to process basal NF-κB signaling. In malignant lung adenocarcinoma cells, high UBE2S expression was bound to IκBα for degradation. p65 and p50 entered nuclei to activate NF-κB signaling.

UBE2S is an E2 ubiquitination ligase and is involved in different signaling pathways during tumorigenesis in many tumor types. UBE2S mediated tumor progression via Sox6/β-catenin signaling in endometrial cancer [45], was associated with malignant properties of breast cancer [46], enhanced ubiquitination of p53 to exert oncogenic activities in hepatocellular carcinoma [47], was mediated by VHL/Hif1α/Stat3 signaling to promote EMT signaling [43], and promoted the proliferation and survival of lung adenocarcinoma cells by activating multiple gene expressions [14]. In our earlier report, UBE2S activated the migration and invasion of squamous cell carcinoma cells through EMT signaling [28]. Although UBE2S is involved in tumorigenesis of multiple tumors, the detailed mechanism is still unclear. In this study, we showed novel non-canonical activation of NF-κB signaling by UBE2S which promoted the metastasis of adenocarcinoma cells. This finding provides an important function of UBE2S in regulating and activating NF-κB signaling in lung adenocarcinomas. Therefore, we did not provide the distinct binding position of UBE2S and IκBα; the PEST domain of the C-terminal region of IκBα, which was suggested to be a binding region of free IκBα for degradation [24], might be a potential site for UBE2S binding for degradation. This suggestion requires further investigation.

NF-κB signaling was reported to regulate cancer progression in multiple cancers. High constitutive NF-κB activity and low IκBα expression were found in some cancer cell lines [48, 49]. Phosphorylation and degradation of IκBα by IKK to activate NF-κB signaling constitute the canonical pathway. The non-canonical NF-κB pathway might not involve degradation of IκBα and may be regulated by p100 [50]. However, a report showed that NF-κB signaling was activated in IKK1/2-devoid mouse embryo fibroblasts. Degradation of IκBα was induced by doxorubicin-induced DNA damage and was inhibited by the phosphatidylinositol 3-kinase inhibitor, LY294002 [51]. In a previous report, UBE2S was regulated by Akt and was associated with the DNA damage response by the Ku70 complex [10]. In our present data, Ly294002 reduced protein levels of UBE2S and increased IκBα in lung adenocarcinoma cells. Knockdown and overexpression of UBE2S in adenocarcinoma cells increased nuclear entry of p65 and activated the transactivation activity of the NF-κB reporter. This activation further induced EMT signaling and metastasis of lung adenocarcinoma cells in zebrafish xenograft tumor model. These results showed a new tumor progression mechanism, and UBE2S might be a new therapeutic target in lung adenocarcinoma.

Conclusions

UBE2S in lung adenocarcinoma patients was negatively related to the survival rate. Higher UBE2S expressed in lung adenocarcinomas was directly binding with IκBα to activate NF-κB signaling. The downstream EMT signaling was activated to promote metastasis of cancer cells. UBE2S might be a potential therapeutic target for lung adenocarcinomas.

Declarations

Ethics approval and consent to participate

Not applicable.

Consent for publication

Not applicable.

Availability of data and materials

Not applicable.

Conflict of interests

The authors declare that they have no conflicts of interest.

Funding

This work was financially supported by the Higher Education Sprout Project of the Ministry of Education (MOE), Taiwan (DP2-109-21121-03-C-03-04).

Authors' contributions

Chia-Hsiung Cheng designed this research. Jhih-Yun Ho, Hsing-Hsien Cheng, and Yu-Chieh Kuo performed the experiments and analyzed the data. Yu-Lin Amy Lee helped with manuscript preparation.

Acknowledgements

We thank the Zebrafish Core Facility of Taipei Medical University for providing technical supports.

References

1. Bremm A, Komander D. Emerging roles for Lys11-linked polyubiquitin in cellular regulation. Trends Biochem Sci. 2011;36(7):355–63.
2. Bremm A, Komander D. Synthesis and analysis of K11-linked ubiquitin chains. Methods in molecular biology. 2012;832:219–28.

3. Wickliffe KE, Lorenz S, Wemmer DE, Kuriyan J, Rape M. The mechanism of linkage-specific ubiquitin chain elongation by a single-subunit E2. Cell. 2011;144(5):769–81.
4. Schwartz AL, Ciechanover A. The ubiquitin-proteasome pathway and pathogenesis of human diseases. Annual review of medicine. 1999;50:57–74.
5. Chen MF, Lee KD, Lu MS, Chen CC, Hsieh MJ, Liu YH, Lin PY, Chen WC. The predictive role of E2-EPF ubiquitin carrier protein in esophageal squamous cell carcinoma. Journal of molecular medicine. 2009;87(3):307–20.
6. Tedesco D, Zhang J, Trinh L, Lalehzadeh G, Meisner R, Yamaguchi KD, Ruderman DL, Dinter H, Zajchowski DA. The ubiquitin-conjugating enzyme E2-EPF is overexpressed in primary breast cancer and modulates sensitivity to topoisomerase II inhibition. Neoplasia. 2007;9(7):601–13.
7. Liang J, Nishi H, Bian ML, Higuma C, Sasaki T, Ito H, Isaka K. The ubiquitin-conjugating enzyme E2-EPF is overexpressed in cervical cancer and associates with tumor growth. Oncol Rep. 2012;28(4):1519–25.
8. Roos FC, Evans AJ, Brenner W, Wondergem B, Klomp J, Heir P, Roche O, Thomas C, Schimmel H, Furge KA, et al. Deregulation of E2-EPF ubiquitin carrier protein in papillary renal cell carcinoma. Am J Pathol. 2011;178(2):853–60.
9. Lin M, Lei T, Zheng J, Chen S, Du L, Xie H. UBE2S mediates tumor progression via SOX6/beta-Catenin signaling in endometrial cancer. Int J Biochem Cell Biol. 2019;109:17–22.
10. Hu L, Li X, Liu Q, Xu J, Ge H, Wang Z, Wang H, Wang Z, Shi C, Xu X, et al. UBE2S, a novel substrate of Akt1, associates with Ku70 and regulates DNA repair and glioblastoma multiforme resistance to chemotherapy. Oncogene. 2017;36(8):1145–56.
11. Li Z, Wang Y, Li Y, Yin W, Mo L, Qian X, Zhang Y, Wang G, Bu F, Zhang Z, et al. Ube2s stabilizes beta-Catenin through K11-linked polyubiquitination to promote mesendoderm specification and colorectal cancer development. Cell Death Dis. 2018;9(5):456.
12. Hosseini SM, Okoye I, Chaleshtari MG, Hazhirkarzar B, Mohamadnejad J, Azizi G, Hojjat-Farsangi M, Mohammadi H, Shotorbani SS, Jadidi-Niaragh F. E2 ubiquitin-conjugating enzymes in cancer: Implications for immunotherapeutic interventions. Clin Chim Acta. 2019;498:126–34.
13. Jung CR, Hwang KS, Yoo J, Cho WK, Kim JM, Kim WH, Im DS. E2-EPF UCP targets pVHL for degradation and associates with tumor growth and metastasis. Nature medicine. 2006;12(7):809–16.
14. Liu Z, Xu L. UBE2S promotes the proliferation and survival of human lung adenocarcinoma cells. BMB Rep. 2018;51(12):642–7.
15. Gu L, Wang Z, Zuo J, Li H, Zha L: **Prognostic significance of NF-kappaB expression in non-small cell lung cancer: A meta-analysis**. *PLoS One* 2018, **13**(5):e0198223.
16. Viatour P, Merville MP, Bours V, Chariot A. Phosphorylation of NF-kappaB and IkappaB proteins: implications in cancer and inflammation. Trends Biochem Sci. 2005;30(1):43–52.
17. Cao Y, Bonizzi G, Seagroves TN, Greten FR, Johnson R, Schmidt EV, Karin M. IKKα Provides an Essential Link between RANK Signaling and Cyclin D1 Expression during Mammary Gland

Development. Cell. 2001;107(6):763–75.
18. Karin M, Lin A. NF-kappaB at the crossroads of life and death. Nat Immunol. 2002;3(3):221–7.
19. Webster GA, Perkins ND. Transcriptional cross talk between NF-kappaB and p53. Mol Cell Biol. 1999;19(5):3485–95.
20. Wang CY, Cusack JC Jr, Liu R, Baldwin AS Jr. Control of inducible chemoresistance: enhanced anti-tumor therapy through increased apoptosis by inhibition of NF-kappaB. Nature medicine. 1999;5(4):412–7.
21. Takeshita H, Yoshizaki T, Miller WE, Sato H, Furukawa M, Pagano JS, Raab-Traub N. Matrix metalloproteinase 9 expression is induced by Epstein-Barr virus latent membrane protein 1 C-terminal activation regions 1 and 2. J Virol. 1999;73(7):5548–55.
22. Bond M, Fabunmi RP, Baker AH, Newby AC. Synergistic upregulation of metalloproteinase-9 by growth factors and inflammatory cytokines: an absolute requirement for transcription factor NF-kappa B. FEBS Lett. 1998;435(1):29–34.
23. Dejardin E, Deregowski V, Chapelier M, Jacobs N, Gielen J, Merville MP, Bours V. Regulation of NF-kappaB activity by I kappaB-related proteins in adenocarcinoma cells. Oncogene. 1999;18(16):2567–77.
24. Mathes E, O'Dea EL, Hoffmann A, Ghosh G. NF-kappaB dictates the degradation pathway of IkappaBalpha. EMBO J. 2008;27(9):1357–67.
25. Kao WT, Lin CY, Lee LT, Lee PP, Hung CC, Lin YS, Chen SH, Ke FC, Hwang JJ, Lee MT. Investigation of MMP-2 and – 9 in a highly invasive A431 tumor cell sub-line selected from a Boyden chamber assay. Anticancer research. 2008;28(4B):2109–20.
26. Lin CY, Tsai PH, Kandaswami CC, Lee PP, Huang CJ, Hwang JJ, Lee MT. Matrix metalloproteinase-9 cooperates with transcription factor Snail to induce epithelial-mesenchymal transition. Cancer Sci. 2011;102(4):815–27.
27. Lin CW, Lai GM, Chen KC, Lin TH, Fan JJ, Hsu RL, Chou CM, Lin CM, Kandaswami CC, Lee MT, et al. RPS12 increases the invasiveness in cervical cancer activated by c-Myc and inhibited by the dietary flavonoids luteolin and quercetin. J Funct Foods. 2015;19:236–47.
28. Lin TH, Hsu WH, Tsai PH, Huang YT, Lin CW, Chen KC, Tsai IH, Kandaswami CC, Huang CJ, Chang GD, et al. Dietary flavonoids, luteolin and quercetin, inhibit invasion of cervical cancer by reduction of UBE2S through epithelial-mesenchymal transition signaling. Food Funct. 2017;8(4):1558–68.
29. Chen KC, Hsu WH, Ho JY, Lin CW, Chu CY, Kandaswami CC, Lee MT, Cheng CH. Flavonoids Luteolin and Quercetin Inhibit RPS19 and contributes to metastasis of cancer cells through c-Myc reduction. J Food Drug Anal. 2018;26(3):1180–91.
30. Fan JJ, Hsu WH, Lee KH, Chen KC, Lin CW, Lee YA, Ko TP, Lee LT, Lee MT, Chang MS, et al: **Dietary Flavonoids Luteolin and Quercetin Inhibit Migration and Invasion of Squamous Carcinoma through Reduction of Src/Stat3/S100A7 Signaling**. *Antioxidants (Basel)* 2019, **8**(11):557–573.
31. Malaguarnera R, Belfiore A. The emerging role of insulin and insulin-like growth factor signaling in cancer stem cells. Front Endocrinol (Lausanne). 2014;5:10.

32. Lin CY, Tsai PH, Kandaswami CC, Chang GD, Cheng CH, Huang CJ, Lee PP, Hwang JJ, Lee MT. Role of tissue transglutaminase 2 in the acquisition of a mesenchymal-like phenotype in highly invasive A431 tumor cells. Mol Cancer. 2011;10:87.
33. Tsai PH, Cheng CH, Lin CY, Huang YT, Lee LT, Kandaswami CC, Lin YC, Lee KP, Hung CC, Hwang JJ, et al. Dietary Flavonoids Luteolin and Quercetin Suppressed Cancer Stem Cell Properties and Metastatic Potential of Isolated Prostate Cancer Cells. Anticancer Res. 2016;36(12):6367–80.
34. Fan JJ, Hsu WH, Hung HH, Zhang WJ, Lee YA, Chen KC, Chu CY, Ko TP, Lee MT, Lin CW, et al. Reduction in MnSOD promotes the migration and invasion of squamous carcinoma cells. Int J Oncol. 2019;54(5):1639–50.
35. Tang Z, Kang B, Li C, Chen T, Zhang Z. GEPIA2: an enhanced web server for large-scale expression profiling and interactive analysis. Nucleic Acids Res. 2019;47(W1):W556–60.
36. Uhlen M, Fagerberg L, Hallstrom BM, Lindskog C, Oksvold P, Mardinoglu A, Sivertsson A, Kampf C, Sjostedt E, Asplund A, et al. Proteomics. Tissue-based map of the human proteome. Science. 2015;347(6220):1260419.
37. Bivona TG, Hieronymus H, Parker J, Chang K, Taron M, Rosell R, Moonsamy P, Dahlman K, Miller VA, Costa C, et al. FAS and NF-kappaB signalling modulate dependence of lung cancers on mutant EGFR. Nature. 2011;471(7339):523–6.
38. Chen W, Li Z, Bai L, Lin Y. NF-kappaB in lung cancer, a carcinogenesis mediator and a prevention and therapy target. Front Biosci (Landmark Ed). 2011;16:1172–85.
39. Cai Z, Tchou-Wong KM, Rom WN. NF-kappaB in lung tumorigenesis. Cancers (Basel). 2011;3(4):4258–68.
40. Wu ZH, Shi Y. When ubiquitin meets NF-kappaB: a trove for anti-cancer drug development. Curr Pharm Des. 2013;19(18):3263–75.
41. Dynek JN, Goncharov T, Dueber EC, Fedorova AV, Izrael-Tomasevic A, Phu L, Helgason E, Fairbrother WJ, Deshayes K, Kirkpatrick DS, et al. c-IAP1 and UbcH5 promote K11-linked polyubiquitination of RIP1 in TNF signalling. EMBO J. 2010;29(24):4198–209.
42. Huber MA, Azoitei N, Baumann B, Grunert S, Sommer A, Pehamberger H, Kraut N, Beug H, Wirth T. NF-kappaB is essential for epithelial-mesenchymal transition and metastasis in a model of breast cancer progression. J Clin Invest. 2004;114(4):569–81.
43. Wang L, Liang Y, Li P, Liang Q, Sun H, Xu D, Hu W. Oncogenic Activities Of UBE2S Mediated By VHL/HIF-1alpha/STAT3 Signal Via The Ubiquitin-Proteasome System In PDAC. Onco Targets Ther. 2019;12:9767–81.
44. Hsu WJ, Lin MH, Kuo TC, Chou CM, Mi FL, Cheng CH, Lin CW. Fucoidan from Laminaria japonica exerts antitumor effects on angiogenesis and micrometastasis in triple-negative breast cancer cells. Int J Biol Macromol. 2020;149:600–8.
45. Hung KC, Huang TC, Cheng CH, Cheng YW, Lin DY, Fan JJ, Lee KH. The Expression Profile and Prognostic Significance of Metallothionein Genes in Colorectal Cancer. Int J Mol Sci. 2019;20(16):3849–60.

46. Ayesha AK, Hyodo T, Asano E, Sato N, Mansour MA, Ito S, Hamaguchi M, Senga T. UBE2S is associated with malignant characteristics of breast cancer cells. Tumour Biol. 2016;37(1):763–72.
47. Pan YH, Yang M, Liu LP, Wu DC, Li MY, Su SG. UBE2S enhances the ubiquitination of p53 and exerts oncogenic activities in hepatocellular carcinoma. Biochem Biophys Res Commun. 2018;503(2):895–902.
48. Taniguchi K, Karin M. NF-kappaB, inflammation, immunity and cancer: coming of age. Nat Rev Immunol. 2018;18(5):309–24.
49. Karin M. How NF-kappaB is activated: the role of the IkappaB kinase (IKK) complex. Oncogene. 1999;18(49):6867–74.
50. Shin CH, Choi DS. **Essential Roles for the Non-Canonical IkappaB Kinases in Linking Inflammation to Cancer, Obesity, and Diabetes**. *Cells* 2019, 8(2).
51. Tergaonkar V, Bottero V, Ikawa M, Li Q, Verma IM. IkappaB kinase-independent IkappaBalpha degradation pathway: functional NF-kappaB activity and implications for cancer therapy. Mol Cell Biol. 2003;23(22):8070–83.
52. Lee WY, Chen PC, Wu WS, Wu HC, Lan CH, Huang YH, Cheng CH, Chen KC, Lin CW. Panobinostat sensitizes KRAS-mutant non-small-cell lung cancer to gefitinib by targeting TAZ. Int J Cancer. 2017;141(9):1921–31.
53. Cheng CH, Chou CM, Chu CY, Chen GD, Lien HW, Hwang PP, Chang MS, Huang CJ: **Differential regulation of Tetraodon nigroviridis Mx gene promoter activity by constitutively-active forms of STAT1, STAT2, and IRF9**. *Fish Shellfish Immunol* 2014, **38**(1):230–243.
54. Deryckere F, Gannon F. A one-hour minipreparation technique for extraction of DNA-binding proteins from animal tissues. Biotechniques. 1994;16(3):405.
55. Huang CJ, Chou CM, Lien HW, Chu CY, Ho JY, Wu Y, Cheng CH. IRF9-Stat2 Fusion Protein as an Innate Immune Inducer to Activate Mx and Interferon-Stimulated Gene Expression in Zebrafish Larvae. Mar Biotechnol (NY). 2017;19(3):310–9.
56. Lien HW, Yuan RY, Chou CM, Chen YC, Hung CC, Hu CH, Hwang SP, Hwang PP, Shen CN, Chen CL, et al: **Zebrafish cyclin Dx is required for development of motor neuron progenitors, and its expression is regulated by hypoxia-inducible factor 2alpha**. *Sci Rep* 2016, **6**:28297.
57. Lee WT, Lee TH, Cheng CH, Chen KC, Chen YC, Lin CW. Antroquinonol from Antrodia Camphorata suppresses breast tumor migration/invasion through inhibiting ERK-AP-1- and AKT-NF-kappaB-dependent MMP-9 and epithelial-mesenchymal transition expressions. Food chemical toxicology: an international journal published for the British Industrial Biological Research Association. 2015;78C:33–41.

Figures

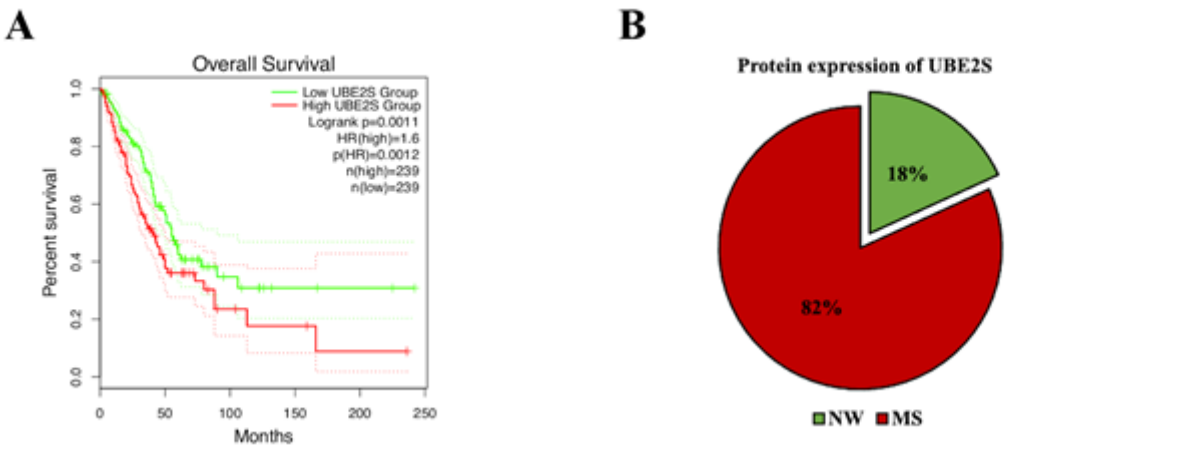

Figure 1

Expression of ubiquitin-conjugating enzyme E2S (UBE2S) in lung adenocarcinoma patients. (A) Kaplan-Meier survival plot of UBE2S from TCGA lung adenocarcinoma (LUAD) patients. (B) Protein levels of UBE2S were classified as normal and weak (NW) or medium and strong (MS) in LUAD patients from the Human Protein Atlas database.

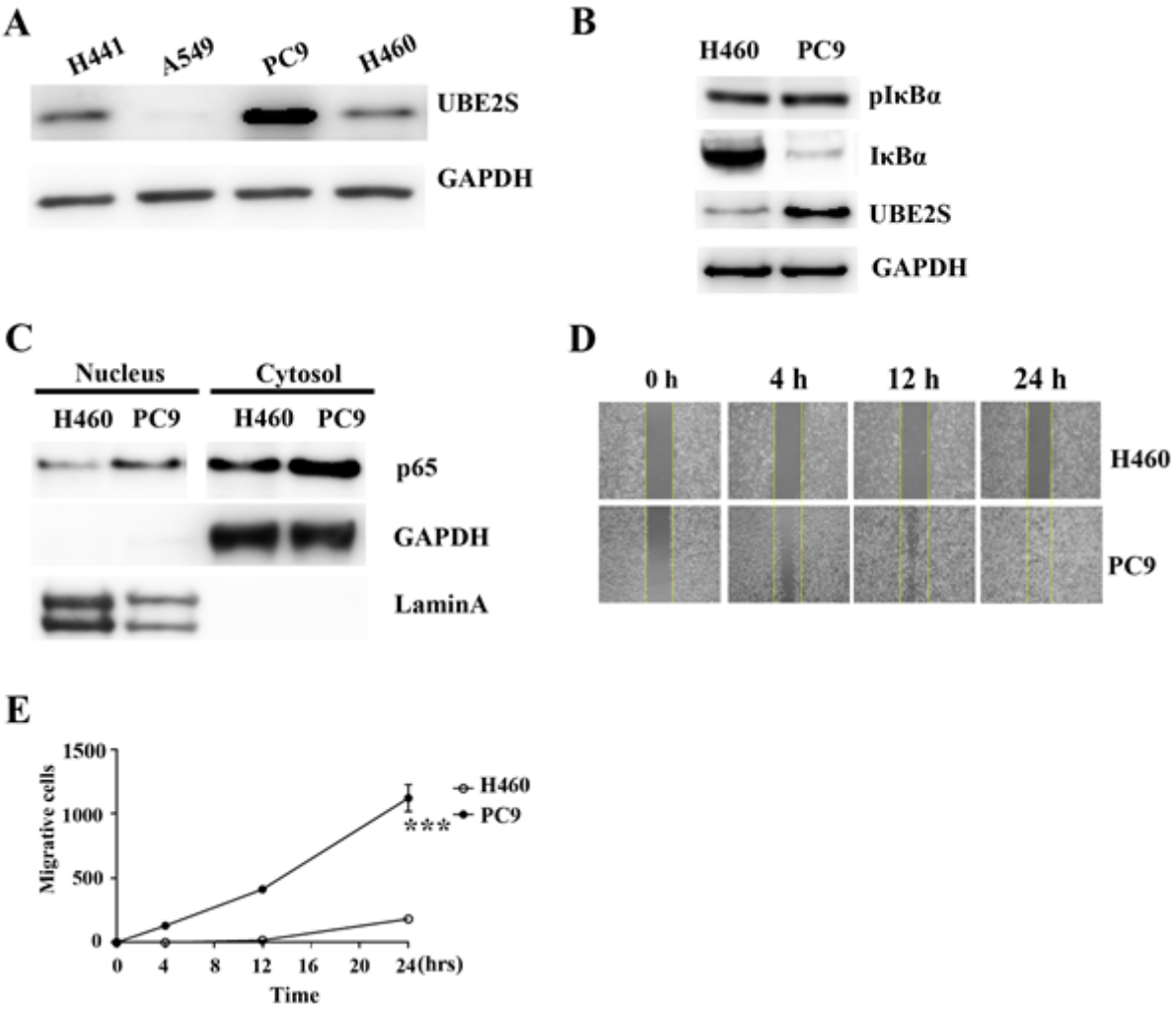

Figure 2

Expression of ubiquitin-conjugating enzyme E2S (UBE2S) in lung adenocarcinoma cells. (A) Protein levels of UBE2S in the H441, A549, PC9, and H460 cell lines. (B) Protein levels of phosphorylated (p)-inhibitor of nuclear factor-κBα (IκBα), IκBα, and UBE2S in H460 and PC9 cells. (C) Protein levels of p65 in the cytosol and nuclei of H460 and PC9 cells. The migratory ability of H460 and PC9 cells was analyzed by a wound-healing assay (D, E). *** Indicates a significant difference compared to the control ($p < 0.001$).

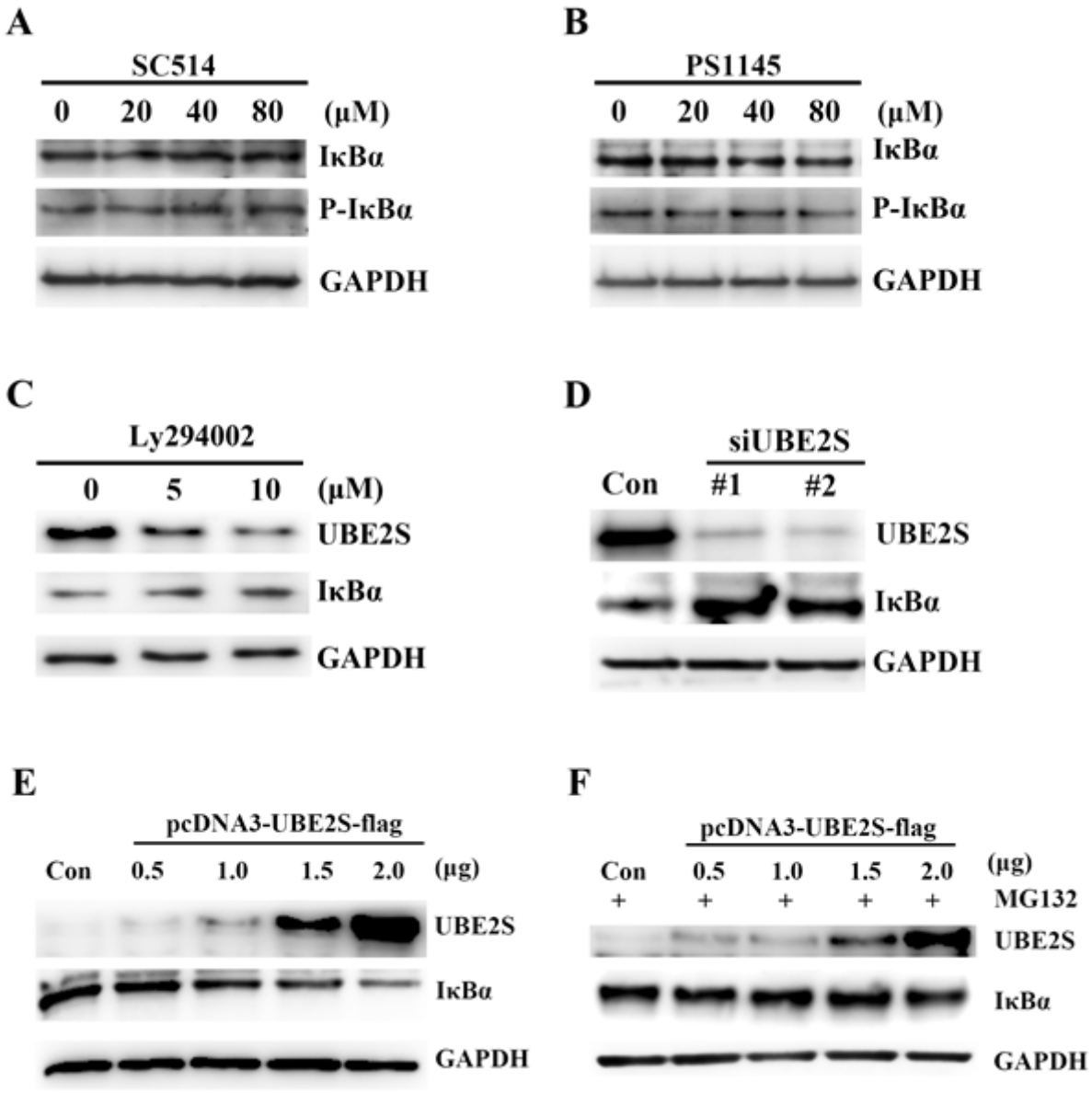

Figure 3

Ubiquitin-conjugating enzyme E2S (UBE2S) regulates inhibitor of nuclear factor-κBα (IκBα) without inhibitor of κB kinase (IKK) activation in lung adenocarcinoma cells. Protein levels of phosphorylated (p)-IκBα and IκBα were analyzed by treatment with SC514 (A) and PS1145 in PC9 cells. Protein levels of IκBα and UBE2S were analyzed by treatment with Ly294002 (C) and knockdown with UBE2S siRNA

(siUBE2S#1 and -#2) or control siRNA (Con) (D) in PC9 cells. (E) Protein levels of IκBα were analyzed by overexpression of UBE2S (E) and co-treatment with MG132 (F) in H460 cells.

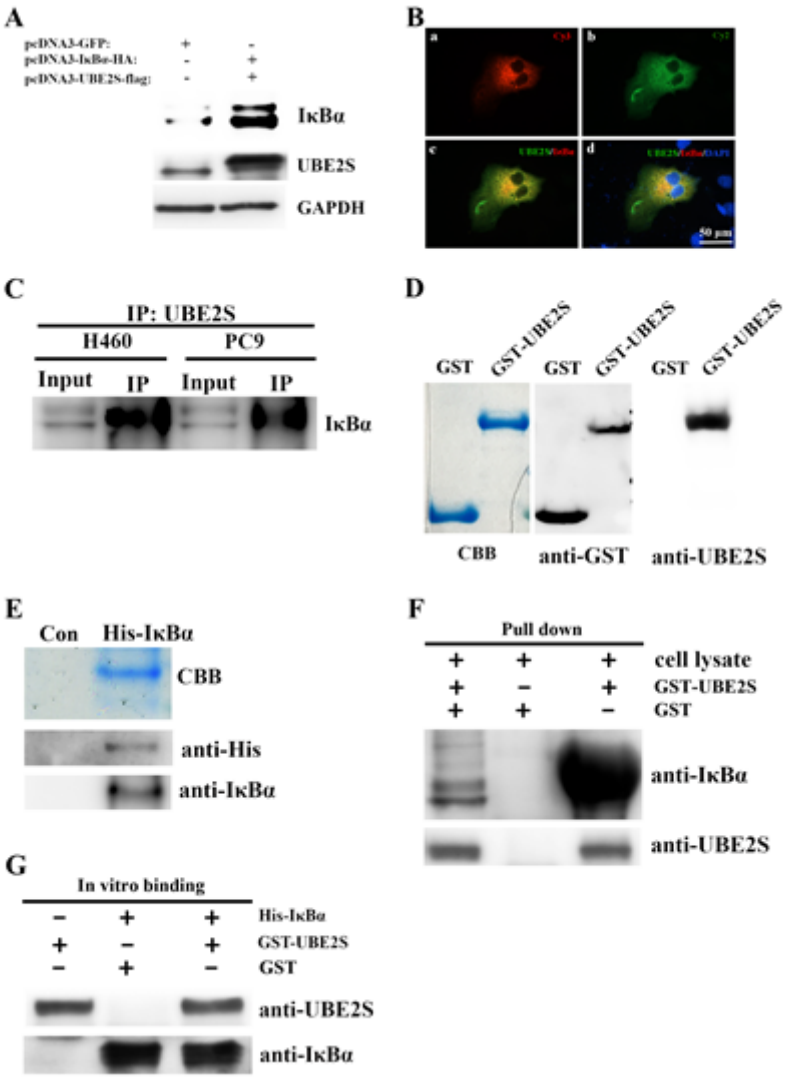

Figure 4

Ubiquitin-conjugating enzyme E2S (UBE2S) directly bound to inhibitor of nuclear factor-κBα (IκBα). (A) Overexpression of UBE2S (pcDNA3-UBE2S-flag) and IκBα (pcDNA3-IκBα-HA) in COS-1 cells was analyzed by Western blotting. (B) Overexpression of UBE2S (green) and IκBα (red) was used to analyze their localization in COS-1 cells by an immunostaining experiment. (C) An immunoprecipitation (IP) assay was used to analyze interactions of UBE2S and IκBα in H460 and PC9 lung cancer cells. Protein levels of glutathione S-transferase (GST), GST-UBE2S (D), and His-IκBα (E) were expressed and purified from E. coli. and analyzed by Coomassie blue (CBB) staining and Western blotting. (F) A GST-pull-down assay was used to analyze the interaction of UBE2S (GST-UBE2S) with IκBα in PC9 cell lysates. (G) An in vitro binding assay was used to analyze the binding of UBE2S (GST-UBE2S) and IκBα (His-IκBα).

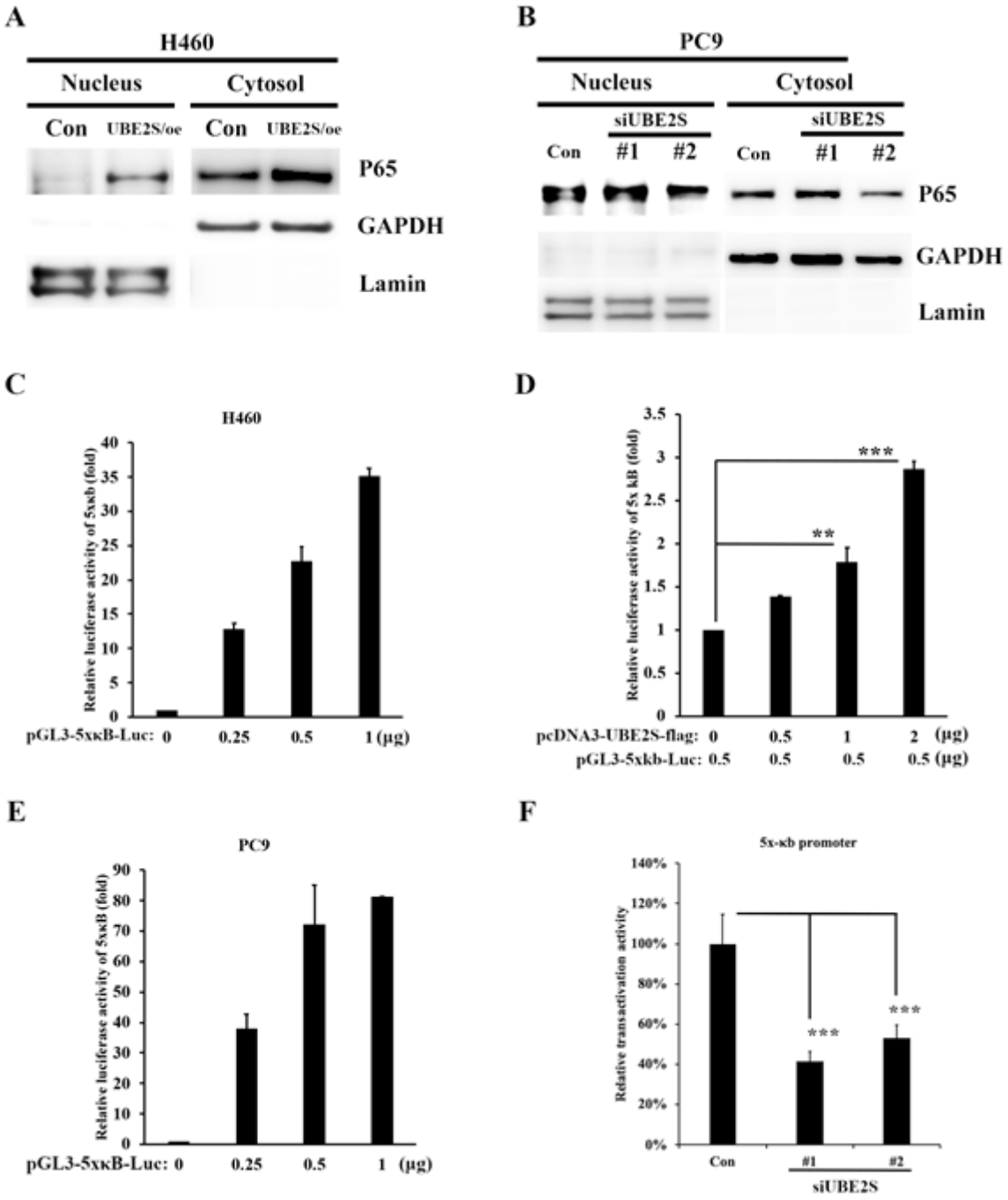

Figure 5

Ubiquitin-conjugating enzyme E2S (UBE2S) activates epithelial-to-mesenchymal transition (EMT) signaling through nuclear factor (NF)-κB signaling. UBE2S was overexpressed (UBE2S o/e) in H460 cells (A), and it was knocked-down by siRNAs (siUBE2S#1 and -#2) in PC9 cells (B) to analyze p65 protein levels in the cytosol and nuclei. Transactivation activity of the 5x κB promoter in H460 cells (C) and activation by UBE2S overexpression (D) were analyzed. Transactivation activity of the 5x κB promoter in PC9 cells (E) and knockdown by UBE2S siRNA (F) were analyzed.

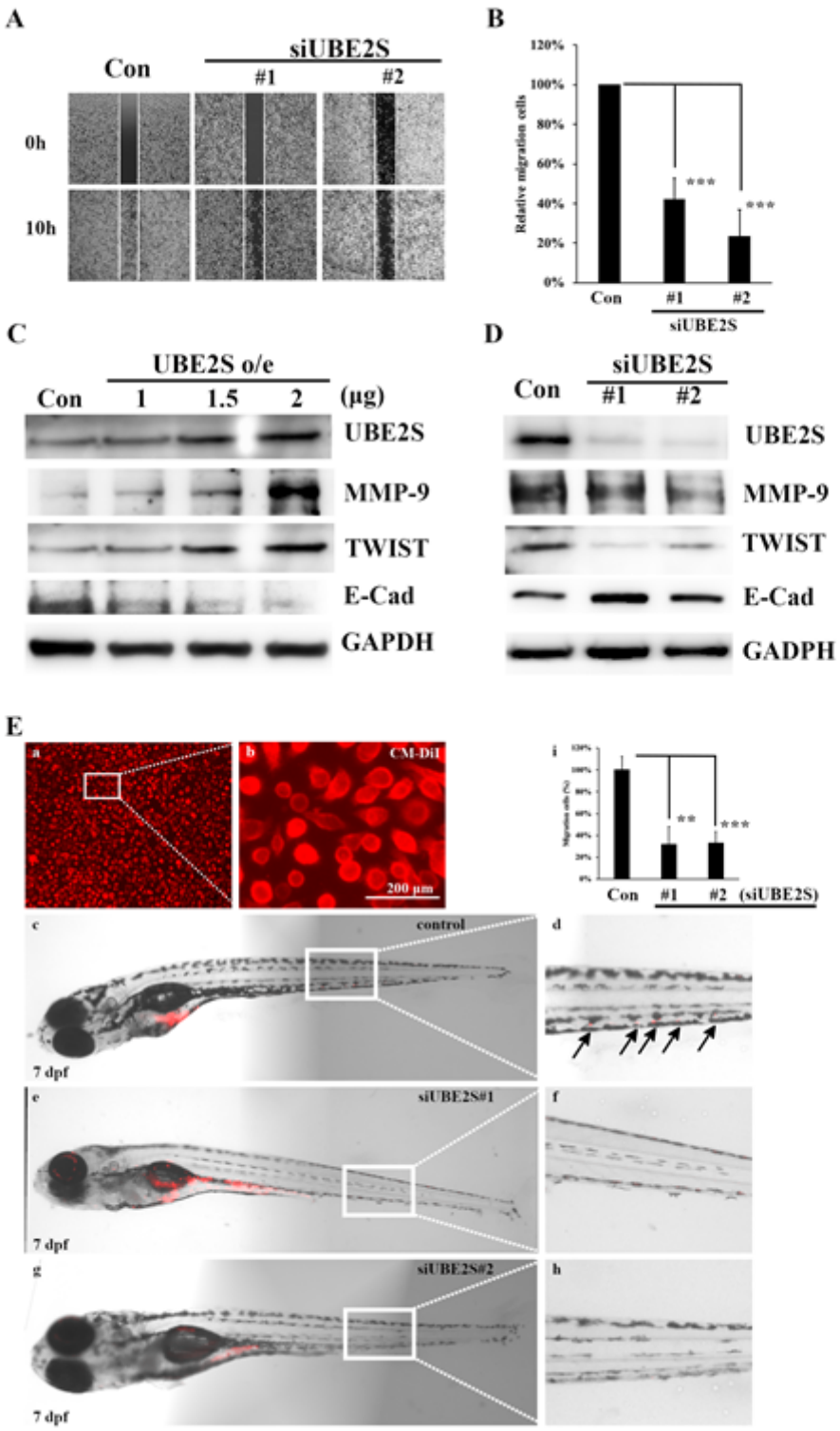

Figure 6

Metastasis of PC9 lung cancer cells was inhibited by knockdown of the ubiquitin-conjugating enzyme E2S (ubiquitin-conjugating enzyme E2S (UBE2S)) siRNA. (A) Migratory activity of PC9 cells was reduced by knockdown with UBE2S siRNAs (siUBE2S#1 and -#2). (B) Statistical results of the migratory ability were analyzed from (A). UBE2S was overexpressed (UBE2S o/e) in H460 cells (C), and knockdown by siRNAs (siUBE2S#1 and -#2) in PC9 cells (D) was performed to analyze protein levels of UBE2S, matrix

metalloproteinase (MMP)-9, TWIST, and E-cadherin (E-Cad) by Western blotting. (E) Metastasis analysis of PC9 lung cancer cells in zebrafish larvae. The PC9 cells were stained with CM-DiI (a-b). PC9 cells knockdown with siUBE2S (e-h) or control siRNA (c-d) were microinjected into 3 dpf zebrafish larvae and then analyzed the migrative PC9 cells at 7 dpf zebrafish larvae. (i) Statistical analysis of metastatic PC9 cells in zebrafish larvae by knockdown with control (control) and UBE2S siRNA (siUBE2S#1, #2).

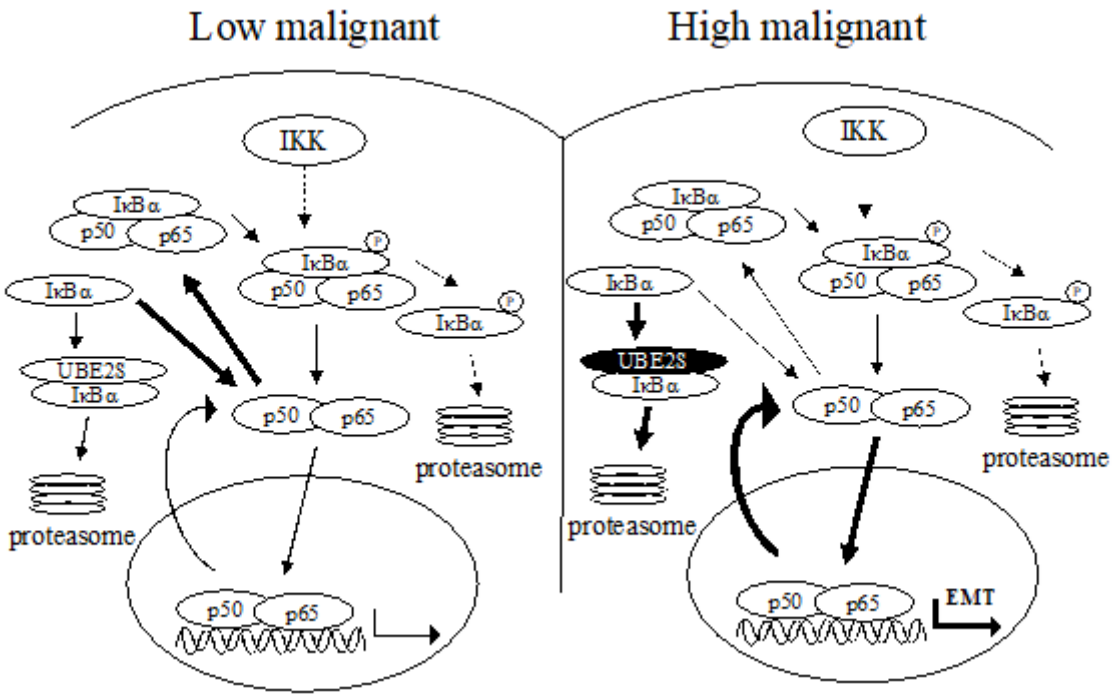

Figure 7

UBE2S activated nuclear factor (NF)-κB signaling in lung adenocarcinomas. In low-malignancy lung adenocarcinoma cells, low ubiquitin-conjugating enzyme E2S (UBE2S) expression failed to bind with inhibitor of nuclear factor-κBα (IκBα) for degradation. IκBα was bound with p65 and p50. Weak inhibitor of κB kinase (IKK) signaling was activated to process basal NF-κB signaling. In malignant lung adenocarcinomas, high UBE2S expression was bound with IκBα for degradation, then p65 and p50 entered nuclei to activate NF-κB signaling.